Met. Mater. Int., Vol. 22, No. 4 (2016), pp. 551~556
doi: 10.1007/s12540-016-6034-5

Phase Evolution, Microstructure and Mechanical Properties of Equi-Atomic Substituted TiZrHfNiCu and TiZrHfNiCuM (M = Co, Nb) High-Entropy Alloys

Hae Jin Park[1], Young Sang Na[2], Sung Hwan Hong[1], Jeong Tae Kim[1], Young Seok Kim[1], Ka Ram Lim[2], Jin Man Park[3,*], and Ki Buem Kim[1,*]

[1]Department of Nanotechnology and Advanced Materials Engineering, Sejong University, Seoul 05006, Republic of Korea
[2]Light Metal Division, Korea Institute of Materials Science(KIMS), Changwon 51508, Republic of Korea
[3]Global Production Technology Center, Samsung Electronics Co., LTD, Suwon 16678, Republic of Korea

(received date: 11 January 2016 / accepted date: 28 January 2016)

In this study, alloys with composition of equi-atomic substituted TiZrHfNiCu, TiZrHfNiCuCo, and TiZrHfNiCuNb high-entropy alloys (HEAs) were produced by suction casting method. The effects of addition elements on phase composition, microstructure and mechanical behaviors of the HEA were studied. The suction casted $Ti_{20}Zr_{20}Hf_{20}Ni_{20}Cu_{20}$ HEA exhibits single C14 Laves phase ($MgZn_2$-type) with fine homogeneous microstructure. When Co or Nb elements are added, morphologies are slightly modulated toward well-developed dendritic microstructure, phase constitutions are significantly changed from single Laves phase to mixed multi-phases as well as mechanical properties are also altered with increased plasticity and high strength. It is believed that modulated mechanical properties are mainly ascribed to the change of phase constitution and crystalline structure, together with the microstructural characteristics. This clearly reveals that the selection and addition of supplementary elements based on the formation rule for HEAs play an important role on the evolution of phase, microstructural morphology and mechanical properties of $Ti_{20}Zr_{20}Hf_{20}Ni_{20}Cu_{20}$ HEA.

Keywords: alloys, casting, microstructure, mechanical properties, high entropy alloys (HEAs)

1. INTRODUCTION

In general, the traditional strategy for developing metallurgical alloys has been based on only one principal element as the matrix [1-3]. These conventional alloys feature a single principal constituent with minor element mixed in, and often depend on the presence and characteristics of second phase for mechanical properties [4,5]. Therefore, this conventional micro-alloying concept might be limited for the wide evolution of special microstructures and physical/mechanical properties because of limited number of applicable alloy systems [6-13].

Recently, as a progress in advanced metallic materials a new paradigm of metallurgical alloys has been yielded, so-called "high entropy alloys" (HEAs) [14-16]. They are defined as multi-component alloys having at least 5 major metal elements with each elemental atomic ratio between 5 and 35% rather than one dominant one, and all the constituent elements are mixed in equi-atomic or near equi-atomic ratios [15]. Due to the distinct design concept, they exhibit unusual properties [17-20]. Basic idea for alloy design is that the configurational entropy increases with the number of elements. These alloys solidified simple solid solution phases which are stabilized by significant high entropy of mixing in spite of containing multiple elements with different crystal structure. Surprisingly, they show high strength, large ductility, toughness and damage tolerance at room temperature, high temperature as well as cryogenic temperature [21-24].

In this study, we choose the firstly reported $Ti_{20}Zr_{20}Hf_{20}Ni_{20}Cu_{20}$ HEA with bulk glass forming ability of 1.5 mm diameter, exhibiting high compressive fracture strength of 1920 MPa [25]. Based on the understanding of formation rule for HEAs, we designed the HEAs in TiZrHfNiCu system using equi-atomic substitution strategy and explore the microstructure and mechanical properties of suction casted TiZrHfNiCu and TiZrHfNiCuM (M = Co or Nb) HEAs with 2 mm diameter. In addition, the underlying mechanisms associated with the formation rule of HEAs will be discussed using the thermodynamic and topological approaches.

*Corresponding author: jinman_park@hotmail.com, kbkim@sejong.ac.kr

2. EXPERIMENTAL PROCEDURES

The equi-atomic substituted $Ti_{20}Zr_{20}Hf_{20}Ni_{20}Cu_{20}$ and $Ti_{16.667}Zr_{16.667}Hf_{16.667}Ni_{16.667}Cu_{16.667}M_{16.667}$ (M = Co or Nb) alloys were prepared by vacuum arc melting the mixture of high purity element (more than 99.9% purity) under a Ti-gettered argon atmosphere. To ensure homogeneity of the samples, each ingot was reversed and re-melted at least four times. The ingots were then re-melted in a quartz tube and injection into a water-cooled copper mould of 2 mm diameter in an inert gas atmosphere. The crystalline structures of the rods were examined by X-ray diffraction (XRD: D/MAX-2500/PC) using Cu Kα radiation. The microstructure and chemical composition of the alloys were analyzed by scanning electron microscopy (SEM: JEOL JSM-6390) with energy dispersive spectrometry (EDS). The mechanical properties of the specimens with a 2:1 aspect ratio were measured at room temperature under compressive mode at a strain rate of $1\times10^{-3}s^{-1}$.

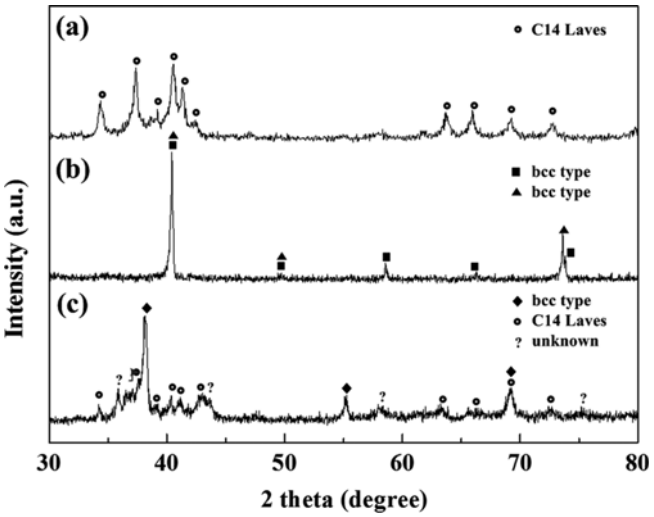

Fig. 1. XRD patterns obtained from the suction-casted (a) TiZrHfNiCu, (b) TiZrHfNiCuCo, and (c) TiZrHfNiCuNb HEAs.

3. RESULTS AND DISCUSSION

Figure 1 shows the X-ray diffraction pattern of the suction-casted TiZrHfNiCu and TiZrHfNiCuM (M = Co or Nb) HEAs. As shown in Fig. 1(a), the diffraction peaks of the TiZrHfNiCu alloy with equi-atomic ratio are composed of intermetallic ($MgZn_2$-type C14 Laves) phase. When Co or Nb elements with equi-atomic ratio are added, the crystalline structures of constituent phases are critically changed. For TiZrHfNiCuCo HEA, several diffraction peaks corresponding to two kinds of bcc-type phases are observed. On the other hand, TiZrHfNiCuNb HEA shows the mixture structure consisting of bcc type phase, intermetallic ($MgZn_2$-type C14 Laves) phase, and unknown phase.

Figure 2 shows SEM backscattering electron (BSE) micrographs of suction-casted TiZrHfNiCu and TiZrHfNiCuM (M = Co or Nb) HEAs. The EDS analysis of as-cast samples is listed in Table 1. The cross-sectional morphologies of currently investigated alloys display a typical dendritic microstructure. As depicted in Fig. 2(a), TiZrHfNiCu HEA shows homogeneous and fine scale microstructure. The average spanning length of dendrite is in the range of 0.5 ~ 1 μm. Co containing TiZrHfNiCu HEA clearly presents further developed dendritic morphology consisting of CoHf-rich and ZrCu-rich phases [Fig. 2(b)]. The average dendrite arm spacing is about ~5μm. The matrix area with dark contrast reveals relatively Cu, Zr and Ti-rich composition. Figure 2(c) shows microstructure of TiZrHfNiCuNb HEA displaying the morphology of columnar dendrites which is composed of Nb-rich phase (gray contrast), C14-type intermetallic phase (bright contrast) and unknown phases (dark contrast). Based on the XRD and EDS analyses, well developed coarse dendrites with dark contrast reveals Nb rich phase, whereas dendrites with bright contrast indicates HfNiCu-rich phase. The composition of interdendritic area is enriched in Ti- , Zr- and Cu-elements [26].

Figure 3 shows the room temperature compressive stress-strain curves of suction-casted (a) TiZrHfNiCu and (b)-(c) TiZrHfNiCuM (M = Co or Nb) HEAs. All samples display high yield strength, fracture strength and moderate plasticity compared with crystalline alloys or Ti-based bulk metallic glasses (BMGs) [27,28]. The values of fracture strength (σ_{max}), yield strength (σ_y) and plastic strain (ε_p) of these alloys are summarized in Fig. 3 (inset image). As shown in Fig. 3(a), the

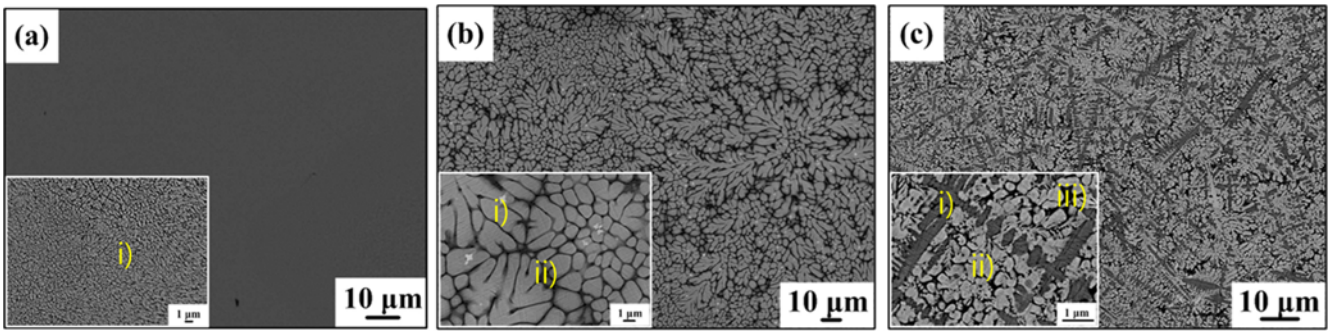

Fig. 2. Backscattered electron SEM micrographs of the suction-casted (a) TiZrHfNiCu, (b) TiZrHfNiCuCo, and (c) TiZrHfNiCuNb HEAs.

Table 1. Average chemical compositions for constituent phases observed in suction casted TiZrHfNiCu, TiZrHfNiCu(Co, Nb) HEAs with equi-atomic substitution ratio, respectively

Alloys	Regions	Ti	Zr	Hf	Ni	Cu	Co	Nb
TiZrHfNiCu	i)	18.898	18.2545	20.857	21.085	20.906	-	-
TiZrHfNiCuCo	i)	15.464	15.288	16.825	18.464	13.629	20.33	-
	ii)	20.854	27.139	7.890	13.326	25.475	5.318	-
TiZrHfNiCuNb	i)	16.727	7.648	11.603	2.682	3.052	-	58.288
	ii)	13.790	18.189	19.277	22.958	20.182	-	5.603
	iii)	25.765	20.844	13.585	14.243	20.964		4.600

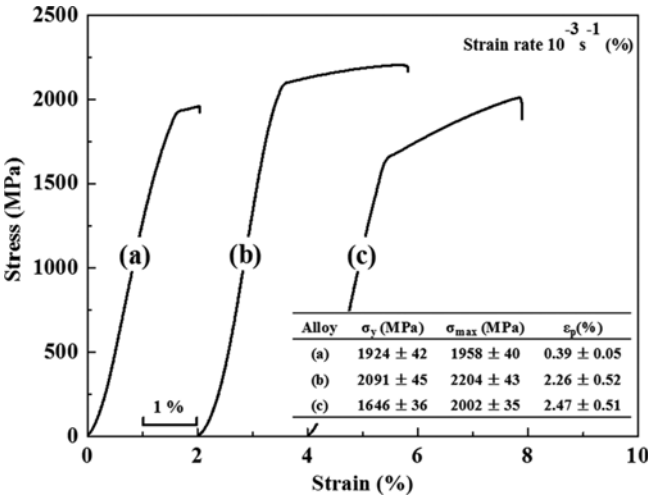

Fig. 3. Compressive stress-strain curves obtained from suction-casted (a) TiZrHfNiCu, (b) TiZrHfNiCuCo, and (c) TiZrHfNiCuNb HEAs.

TiZrHfNiCu alloy exhibits high strength of 1958 MPa and limited plastic strain of 0.4%, respectively. When Co element was added [Fig. 3(b)], improved mechanical properties can be achieved with high yield strength, fracture strength and plasticity of 2224 MPa, 2258 MPa, 2.3%, respectively. For Nb containing alloy, Fig. 3(c) reveals that the addition of Nb further increases the plasticity (2.5%), but deteriorates the yield strength (1646 MPa). Based on the above results, it is supposed that modulated mechanical properties are mainly attributed to the change of phase constitution and crystalline structure, together with the microstructural characteristics. In particular, newly-formed simple cubic symmetry structured intermetallic phase or solid solution phase derived from alloy design employing the phase formation rule for HEAs play a crucial role on the mechanical and deformation behaviors. Therefore, macroscopic mechanical properties of equi-atomic substituted TiZrHfNiCu HEA can be properly optimized with high strength and enhanced plasticity by selection and addition of alloying elements (Co or Nb).

According to the rule of phase formation, the atomic size difference δ and mixing enthalpy ΔH_{mix} are important factor to predict the formation of solid solution phase in multicomponent alloys. Here, the parameter δ is expressed as [29,30]

Table 2. The values of average atomic radius, calculated parameters δ and ΔH_{mix} for the equi-atomic substituted TiZrHfNiCu, TiZrHfNiCu(Co, Nb) HEAs

Alloy	Average atomic radius (nm)	δ	ΔH_{mix} (kJ·mol^{-1})
TiZrHfNiCu	0.143308	10.320	-27.36
TiZrHfNiCuCo	0.140213	10.780	-29.91
TiZrHfNiCuNb	0.143239	9.411	-20.77

$$\delta = \sqrt{\sum_{i=1}^{n} c_i \left(1 - \frac{r_i}{\bar{r}}\right)^2} \quad (1)$$

where n is the number of the components in an alloy system, c_i is the atomic percent of ith element, r_i is the atomic radius of the ith component, $\bar{r} = \sum_{i=1}^{n} c_i r_i$ is the average atomic radius [3,31]. The value of the average atomic radius of the TiZrHfNiCu and TiZrHfNiCuM (M = Co or Nb) HEAs are summarized in Table 2.

For other parameter the chemical mixing enthalpy ΔH_{mix} is determined as

$$\Delta H_{mix} = \sum_{i=1, i\neq j}^{n} \Omega_{ij} c_i c_j \quad (2)$$

where Ω_{ij} is the regular melt interaction parameter between the ith and the jth elements, and c_j is the atomic percent of the jth component.

Ω_{ij} is the expressed as

$$\Omega_{ij} = 4 \times \Delta H_{AB}^{\text{mix}} \quad (3)$$

where $\Delta H_{AB}^{\text{mix}}$ is the mixing enthalpy of binary liquid alloys based on miedema model [32].

In this study, the parameters δ, and ΔH_{mix} of TiZrHfNiCu and TiZrHfNiCuM (M = Co or Nb) alloys are calculated according to Eq. (1), (2), and (3). The corresponding values of HEAs are listed in Table 2.

Generally, the formation of solid solution phases with simple crystal structures was attributed to their high entropies of mixing which suppresses the formation of intermetallic compound or other equilibrium phases. Alloy chemistry of HEAs is complicated due to the equi-molar concentration of each constituent. Therefore, it is supposed that since each element has the same possibility to occupy the lattice site it arranges

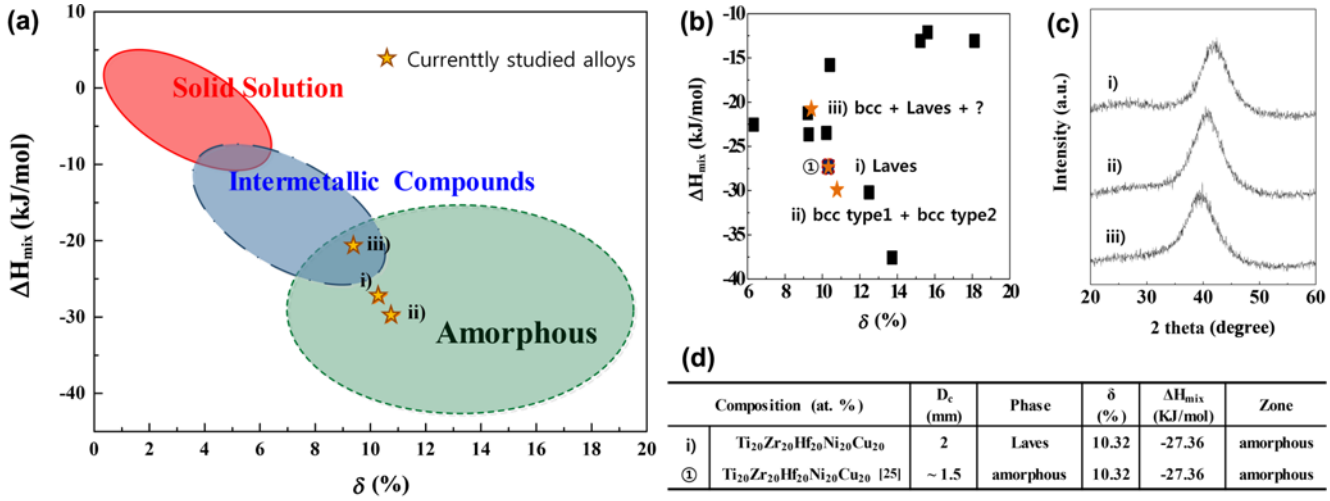

(d)

	Composition (at. %)	D_c (mm)	Phase	δ (%)	ΔH_{mix} (KJ/mol)	Zone
i)	$Ti_{20}Zr_{20}Hf_{20}Ni_{20}Cu_{20}$	2	Laves	10.32	-27.36	amorphous
①	$Ti_{20}Zr_{20}Hf_{20}Ni_{20}Cu_{20}$ [25]	~1.5	amorphous	10.32	-27.36	amorphous

Fig. 4. The phase formation maps (a)-(b) based on the entalpy of mixing ΔH_{mix} and the atomic size difference δ for the formation of solid solution, intermetallic compounds, amorphous phase and XRD data (c) for rapidly quenched TiZrHfNiCu, TiZrHfNiCuM (M = Co, Nb) HEAs: The points and marked zones are for i) TiZrHfNiCu; ii) TiZrHfNiCuCo; iii) TiZrHfNiCuNb HEAs, together with previously developed HEAs. (d) shows the maximum diameter for glass formation, competing crystalline phases, atomic size difference δ, entalpy of mixing ΔH_{mix} and the position in phase formatin map (d).

randomly in the crystal lattices and forms simple solid solutions in multicomponent alloys [33-41]. However, the current studied multicomponent alloys show the formation of mixed multi-phases including intermetallic compound rather than single solid solution phase, though they are designed based on equi-atomic substitution strategy (see Figs. 1 and 2). The formation zone of the i) TiZrHfNiCu, ii) TiZrHfNiCuCo, and iii) TiZrHfNiCuNb HEAs was considered in terms of values of δ and ΔH_{mix}.

Figure 4 illustrates the phase formation zone of the previously developed HEAs and currently studied alloys. From the plots of δ versus ΔH_{mix} for reported HEAs, the HEAs composed of simple single solid solution phase are located in solid solution zone in $\delta < 6.5$ and $-11.6\ \text{kL/mol} < \Delta H_{mix} < 3.2\ \text{kJ/mol}$ [42,43]. In case of equi-atomic substituted TiZrHfNiCu and TiZrHfNiCuM (M = Co or Nb) HEAs, the values of δ and ΔH_{mix} are 10.32, -27.36 kJ/mol, 10.780, -29.91 kJ/mol, 9.411, -20.77 kJ/mol, respectively, and they are located in overlapped area between amorphous zone and intermetallics zone. However, experimental results containing XRD and SEM analyses of suction-casted TiZrHfNiCuM (M = Co or Nb) HEAs demonstrate the formation of single or multi-crystalline phases rather than single amorphous phase (see Fig. 1). Comparing with the experimental and calculation results, it is noted that other critical factor except for δ and ΔH_{mix} can be required to encompass phase formation rule. In this study, suction-casted TiZrHfNiCuM (M = Co or Nb) samples exhibit multi-phase microstructure, whereas rapid quenched melt-spun samples show a single amorphous microstructure (see Figs. 4(b) and (c)) [25]. Due to the fast cooling rate, metastable phase can be formed in the solidified microstructure. Thus the microstructure and phases evolution process may not cause only by composition. This clearly demonstrates that phase constitution of equi-atomic substituted TiZrHfNiCu HEAs located in mixed zone with amorphous and intermetallics can be further altered by control of cooling rate (summarized in Fig. 4(d)) [25]. The presented results demonstrate that the currently studied alloys are composed of complex multi-phases, however, the crystal structure of the observed phases is very different depending on chemical composition i.e., the TiZrHfNiCu alloy is composed of Laves phase, the TiZrHfNiCuCo alloy is composed of two bcc-type phases, and the TiZrHfNiCuNb alloy consists of Laves phase, bcc phase and unknown phase. Apparently, the mechanical properties of the alloys are also strongly affected by their phase composition (see Fig. 3). The effect of composition on phase structure can be simply summarized as "intermetallic vs solid solution vs. amorphous". Apparently, currently studied HEAs even developed based on new alloy designing strategy, are still traditional materials which are different from BMGs without crystalline structure. However, the methods used for producing samples "injection casting into a water-cooled mould" indicating a high cooling rate of the casting process (far from equilibrium) which is similar to BMGs. The fine homogeneous microstructure, as shown in Fig. 2, is attributed to the high cooling rate. Since we investigate the microstructural evolution and mechanical properties of HEAs under relatively rapid quenching casting condition, we further needed to study the mechanical properties and microstructure of these alloy under conventional casting condition in future, as an engineering material. As a result, we demonstrate that phase constitution, microstructure and mechanical properties of equi-atomic substituted TiZrHfNiCu and TiZrHfNiCuM (M = Co, Nb) HEAs can be changed significantly, followed by both the selection of additional elements and the control of cooling rate.

4. CONCLUSIONS

In this study, we deal with investigation of structure and mechanical properties of the TiZrHfNiCu, TiZrHfNiCuCo and TiZrHfNiCuNb high entropy alloys prepared by equi-atomic substitution alloying strategy. The currently studied alloys are composed of predominantly intermetallics or multicrystalline phases and demonstrate high compression strength, yet accompanied by very limited ductility. The conditions for solid solution, intermetallic or amorphous phase formation in high entropy alloys are discussed. The suction-casted equi-atomic $Ti_{20}Zr_{20}Hf_{20}Ni_{20}Cu_{20}$ HEA shows a single Laves phase microstructure exhibiting a high strength of 1958 MPa and limited plasticity of 0.39%. The addition of Co or Nb elements with equi-atomic ratio evolves both the crystalline structure of constituent phases and microstructural morphology, i.e., two kinds of bcc-type phases or mixed multiphase containing sold solution phase are formed and well developed dendritic morphologies are obtained. Furthermore, Co or Nb containing TiZrHfNiCu HEAs show increased plasticity (~2.5%) and high strength (~2258 MPa). These results are mainly attributed to the paucity of multicomponent intermetallic phases with solubility and intersolubility of solid solution in multicomponent alloy. Here we properly select and substitute the constituent elements in TiZrHfNiCu alloy according to the formation rule for HEAs, but we could not obtain single solid solution phase or single amorphous phase. Based on the topological, calculated thermodynamic parameters and experimental constituent phases, it is believed that other factors are also likely to contribute encompass phase formation rule for HEAs except to the atomic radius difference δ and the mixing enthalpy ΔH_{mix}. Particularly, in case of HEAs located in amorphous zone, cooling rate effect also should be considered essentially for phase stability.

ACKNOWLEDGEMENTS

This work was supported by Fundamental Research Program of the Korean Institute of Materials Science (KIMS), the Energy Efficiency & Resources Core Technology Program (No. 20142020103910) and the Human Resources Development of the Korea Institute of Energy and Planning (KETEP) grant funded by the Korea government Ministry of Trade, Industry & Energy (No. 20154030200630).

REFERENCES

1. G. He, J. Eckert, W. G. Loser, and L. Schultz, *Nature* **2**, 33 (2003).
2. A. Inoue, *Bulk Amorphous Alloys: Preparation and Fundamental Characteristics*, p.4, Trans. Tech. Publications, Netherlands (1998).
3. A. Takeuchi and A. Inoue, *Mater. Trans.* **41**, 1372 (2000).
4. H. W. Kui and A. L. Greer, *Appl. Phys. Lett.* **45**, 615 (1984).
5. A. Peker, and W. L. Johnson, *Appl. Phys. Lett.* **63**, 2342 (1993).
6. B.-T. Jang, Y.-I. Kim, and S.-H. Yi, *Korean J. Met. Mater.* **53**, 519 (2015).
7. P. Żywicki, D. H. Ping, T. Abe, H. Garbacz, Y. Yamabe-Mitarai, and K. J. Kurzydłowski, *Met. Mater. Int*. **21**, 617 (2015).
8. B. Cantor, I. T. H. Chang, P. Knight, and A. J. B Vincent, *Mater. Sci. Eng. A* **213**, 375 (2004).
9. B. Cantor, *Encyclopedia of Materials: Sci. Technol.*, 2nd ed., pp.1-3, Elevier, Amsterdam, New York (2001).
10. B. Cantor, *Ann. Chim. Sci. Mater.* **32**, 245 (2007).
11. B. Cantor, K. B. Kim, and P. J. Warren, *Mater. Sci. Forum* **27**, 386 (2002).
12. K. B. Kim, Y. Zhang, P. J. Warren, and B. Cantor, *Philos. Mag.* **83**, 2372 (2003).
13. B. S. Murty, J. W. Yeh, and S. Ranganathan, *High-Entropy Alloys, 1st ed*., pp. 5-12, Butterworth-Heinemann, UK (2014).
14. C. Y. Hsu, J. W. Yeh, S. K. Chen, and T. T. Shun, *Metall. Mater. Trans. A* **35**, 1465 (2004).
15. J. W. Yeh, S. K. Chen, S. J. Lin, J. Y. Gan, T. S. Chin, T. T. Shun, C. H. Tsau, and S. Y. Chang, *Adv. Eng. Mater.* **6**, 299 (2004).
16. J. W. Yeh, *Ann. Chim. Sci. Mater.* **31**, 633 (2006).
17. F. J. Wang, Y. Zhang, and G. L. Chen, *J. Alloy. Compd.* **478**, 321 (2009).
18. V. Dolique, A. L. Thomann, and P. Brault, *J. Mater. Chem. Phys.* **117**, 142 (2009).
19. C. W. Tsai, Y. L. Chen, and M. H. Tsai, *J. Alloys. Compd.* **486**, 427 (2009).
20. C. Y. Hsu, T. S. Shen, and J. W. Yeh, *J. Wear.* **268**, 653 (2012).
21. Y. Y. Chen, T. Duval, and U. D. Hung, *J. Corros. Sci.* **47**, 2257 (2005).
22. Y. J. Zhou, Y. Zhang, and Y. L. Wang, *J. Mater. Sci. Eng. A.* **454**, 260 (2007).
23. Y. S. Huang, L. Chen, and H. W. Lui, *J. Mater. Sci. Eng. A.* **457**, 77 (2007).
24. B. Gludovatz, A. Hohenwarter, D. Catoor, E. H. Chang, E. P. George, and R. O. Ritchie, *Science* **345**, 1153 (2014).
25. L. Ma, L. Wang, T. Zhang, and A. Inoue, *Mater. Trans.* **43**, 277 (2002).
26. A. S. Barros, I. A. Magno, F. A. Souza, C. A. Mota, A. L. Moreira, M. A. Silva, and O. L. Rocha, *Met. Mater. Int*. **21**, 429 (2015).
27. J. M. Park, H. J. Chang, K. H. Han, W. T. Kim, and D. H. Kim, *Scr. Mater.* **53**, 1 (2005).
28. J. M. Park, Y. C. Kim, W. T. Kim and D. H. Kim, *Mater. Trans.* **45**, 595 (2004).
29. G. V. Raynor, *J. Inst. Met.* **98**, 321 (1970).
30. O. N. Senkov and D. B. Miracle, *Mater. Res. Bull.* **36**, 2183 (2001).
31. G. S. James, *Lange's Handbook of Chemistry*, pp. 151-155, McGraw-Hill, New York (2004).
32. F. R. Boer, R. Boom, W. C. M. Mattens, A. R. Miedema, and A. K. Niessen, *Cohesion in Metal*, p. 774, Amsterdam, North-Holland, Netherland (1998).

33. O. N. Senkov, S. V. Senkova, C. Woodward, and D. B. Miracle, *Acta Mater.* **61**, 1545 (2013).
34. É. Fazakas, V. Zadorozhnyy, L. K. Varga, A. Inoue, D. V. Louzguine-Luzgin, F. Tian, and L. Vitos, *Int. J. Ref. Met. Hard Mater.* **47**, 131 (2014).
35. N. D. Stepanov, N. Y. Yurchenko, V. S. Sokolovsky, M. A. Tikhonovsky, and G. A. Salishchev, *Mater Lett.* **161**, 136 (2015).
36. N. D. Stepanov, N. Y. Yurchenko, D. V. Skibin, M. A. Tikhonovsky, and G. A. Salishchev, *J. Alloy. Compd*. **652**, 266 (2015).
37. S. Singh, N. Wanderka, B. S. Murty, U. Glatzel, and J. Banhart, *Acta Mater.* **59**, 182 (2011).
38. D. G. Shaysultanov, N. D. Stepanov, A. V. Kuznetsov, G. A. Salishchev, and O. N. Senkov, *JOM* **65**, 1815 (2013).
39. J. Y. He, W. H. Liu, H. Wang, Y. Wu, X. J. Liu, T. G. Nieh, and Z. P. Lu, *Acta Mater.* **62**, 105 (2014).
40. Y. Lu, Y. Dong, Li. Jiang, T. Wang, T. Li, and Y. Zhang, *Entropy*, **17**, 2355 (2015).
41. T. Dong, Y. Lu, L. Jiang, T. Wang, and T. Li, *Intermetallics* **52**, 105 (2014).
42. S. Guo, Q. Hu, C. Ng, and C. T. Liu, *Intermetallics* **41**, 96 (2013).
43. S. Guo and C. T. Liu, *Prog. Nat. Sci.: Mater. Int.* **21**, 433 (2011).